Article

Programmable Sequences of Reflectin Proteins Provides Evidence for Their Evolution Processes, Tunable Intracellular Localization and Interaction with Cytoskeleton

Junyi Song [1, *, #], Chuanyang Liu[1, #], Baoshan Li[1], Liangcheng Liu[1], Ling Zeng[1], Zonghuang Ye[1], Ting Mao[2], Wenjian Wu [1] and Biru Hu [1,*]

[1] College of Liberal arts Science, National University of Defense Technology, Changsha 410073, China; songjunyi@nudt.edu.cn (J.S.); liuchuanyang13@nudt.edu.cn (C.L.). 1678213718@qq.com (B.L.); 290343303@qq.com (L.L.); zengling14@nudt.edu.cn (L.Z.); yezonghuang15@nudt.edu.cn; (Z.Y.); wjwu67@nudt.edu.cn (W.W.); hubiru08@nudt.edu.cn (B. H)

2 Logistics Center, National University of Defense Technology, Changsha 410073, China; 849281761@qq.com （T.M.）

* Correspondence: songjunyi@nudt.edu.cn; hubiru08@nudt.edu.cn.

[#] These authors contributed equally to this work.

Abstract: Reflectins are membrane-bound proteins located in cephalopods iridocytes, with repeated canonical domains interspersed with cationic linkers. Scientists keep curious about their evolutionary processes, biochemical properties and intracellular functions. Here, by introducing reflectin A1, A2, B1 and C into HEK-293T cells, these proteins were found to phase out from the crowded intracellular milieu, with distinguished localization preferences. Inspired by their programmable block sequences, several truncated reflectin A1 (RfA1) peptides based on repetition of reflectin motifs were designed and transfected into cells. An obvious cyto-/nucleo-plasmic localization preference was once again observed. The dynamic performance of RfA1 derivatives and their analogic behavior between different reflectins suggest a conceivable evolutionary relationship among reflectin proteins. Additionally, a proteomic survey identified biochemical partners which contribute to the phase separation and intracellular localization of RfA1 and its truncations, as well as the close collaboration between RfA1 and the cytoskeleton systems. These findings indicate that liquid-liquid phase separation could be the fundamental mode for reflectins to achieve spatial organization, to cooperate with cytoskeleton during the regulation of reflective coloration. On the other hand, the dynamic behaviors of RfA1 derivatives strongly recommended themselves as programmable molecular tools.

Keywords: reflectins; truncated peptides; phase separation; intracellular localization; protein interaction.

Abbreviations: reflectin (Rf), N-terminal reflectin motif (RM_N), reflectin motifs (RMs), reflectin linkers (RLs), liquid-liquid phase separation (LLPS)

Introduction

Cephalopods (squid, octopus, and cuttlefish) have the remarkable ability to manipulate light to alter their appearance, via the combination of pigmentary and structural elements. Chromatophore organs uppermost in the dermis proportionally regulate coloration by the stretching of pigmentary sacs [1, 2]. While the structural coloration is produced by two classes of cells called iridocytes and leucophores. Distribute at periphery of the iridocytes, Bragg reflectors are periodically stacked lamellae which present iridescence by multilayer interference [3, 4]. Leucophores that contain granular vesicles are responsible for the production of bright white, by unselectively reflecting all visible

light [5].

Interestingly, both the periodically stacked lamellae in iridocytes [3, 4] and the intracellular vesicles in leucophores [6, 7, 8] are unique and composed of reflectin proteins. Reflectin proteins are exclusively expressed in cephalopods, possessing different number of canonical reflectin motifs in different sequential locations [3, 9, 10]. Guan et al. reported that reflectin gene may be traced to a 24-bp transposon-like DNA fragment from the symbiotic bioluminescent bacterium *Vibrio fischeri*[11]. Afterward, million years of self-replication and re-positioning of the transposon leads to the formation of prosperous reflectin family. In *Doryteuthis. Opalescens*, as one representative of the most recently evolved Loliginid species, four distinct reflectins, reflectins A1, A2, B and C, have been identified and characterized [3, 9, 10]. Numerous *in vitro* assays suggested that the dynamic condensation, folding and hierarchical assembly of reflectin proteins play fundamental roles during the formation and regulation of those structural coloration elements in squids [9, 10, 12]. Recently, Daniel E. Morse and his team have preliminarily defined reflectin proteins as a new group of intrinsically disordered proteins (IDPs), and suggested that transient LLPS may dominate reflectin assembly [10]. The dynamic reflectin assembly properties and the intricate reflectin-based biophotonic systems have already inspired the development of various next-generation tunable photonic [13, 14, 15] and electronic platforms and devices[16, 17, 18].

Nevertheless, knowledge about how reflectins molecules are spatially organized to form proteinaceous layers or droplets, and how reflectin manipulates cell membrane and cytoskeleton to fabricate and regulate the Bragg lamellae is still limited.

View from their amino acid sequences, reflectins are block copolymers with repeated canonical domains interspersed with cationic linkers [10], and are fully-prepared IDPs to execute phase separation. Additionally, considering the versatility and importance of LLPS in functional enhancing and structure modulating of its constituents[19, 20], it is reasonable to speculate that reflectin proteins accomplish their spatial enrichment of homogenous molecules via LLPS. This recruitment further accumulates adequate force to interact with membrane and cytoskeleton[21, 22, 23, 24], and ultimately regulates the movement of Bragg lamellae.

Based on this hypothesis, we engineered HEK-293t cells to express either intact RfA1. RfA2, RfB1 or RfC. These proteins are the most widely studied reflectins, with different self-assembly characteristics [10, 12] and membrane-bound properties [25].

Firstly, similar phase separation described by Alon A. Gorodetsky [26] was observed. What is dramatic is the exclusive distribution of RfA1 particles in the cytoplasm, while spherical RfC droplets only existed in the nucleoplasm. As an intermediate state, RfA2 and RfB1 distribute in both cytoplasm and nucleoplasm. It is the first time that the differences among reflectin proteins are displayed in cells, but not in tubes. Then we took the advantage of reflectins programmable sequences and designed a series of RfA1 truncations. By cutting off reflectin motifs (RMs) one by one from RfA1, the length and structure of RfA1 truncations are more and more similar to shorter reflectins. Surprising but reasonable, as the RfA1 derivatives got shorter and shorter, protein droplets gradually change their localization from nucleoplasm to cytoplasm, making them comparable analogs to RfC. CoIP-MS was then employed to decipher the molecular mechanism underlying the phase separation and nuclei importation/exportation of RfA1 and truncations. Cellular components responsible for the facilitation of phase transition and intracellular transportation are identified. Moreover, proteomic analysis also indicated the high affinity of RfA1 to the cytoskeleton, which was further confirmed by confocal observations.

These experimental results indicate omnifarious significances of this study. Firstly, the dynamic performance of RfA1 derivatives and their analogic behavior between shorter reflectins imply the evolutionary order and homology among reflectin proteins. Meanwhile, a rational model is also presented: LLPS is the essential approach employed by reflectin proteins, to recruit a big and strong molecular army; the intimate interaction between RfA1 and cytoskeleton lays the material foundation to establish the Bragg lamellae in iridocytes; the reflectin droplets (as other LLPS products) are sensitive to physiological stimuli, which enables the Bragg lamellae to be dynamic and tunable.

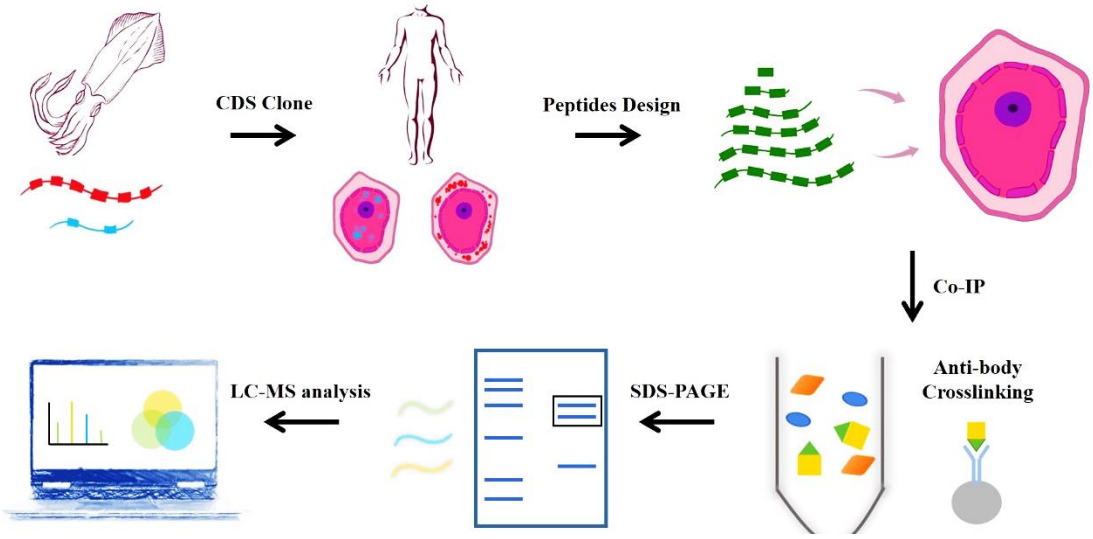

Fig.1 Overview of the workflow. CDS of squids reflectin proteins were obtained from NCBI, optimized according to mammal cell expression preference and introduce into HEK-293T cells by lipofection. RfA1 truncations were designed and cloned into pEGFP-C1 vectors and transfected into HEK293t cells. Anti-GFP mouse monoclonal antibody was used to pull down GFP-tagged RfA1 derivatives and their targeted proteins. The immunoprecipitates were separated using SDS-PAGE, and each gel lanes were digested with trypsin for LC-MS/MS analysis

Results

Phase separation of Reflectin Proteins and their intracellular localization. RfA1, A2, B1 and C possess different numbers and localization of two types of canonical reflectin motifs (Fig. 1a), the regular reflectin motifs (RMs, [M/FD(X)5MD(X)5MDX3/4]) and a N-terminal reflectin motif (RM_N, [MEPMSRM(T/S)- MDF(H/Q)GR(Y/L)(I/M)DS(M/Q)(G/D)R(I/M)VDP(R/G)]) (Fig. 2a). Specifically, RfC is the shortest reflectin, contains a GMXX motif and RM*. The GMXX motif is a unique region of increased overall hydrophobicity composed of a four amino acid repeat, where 'X' represents less conserved locations within the repeat. Asterisk marked RM* of RfC contains substantial deviations in sequence not observed in any other reflectin motifs [27] (Fig. 2b). The disorder tendency of these proteins was calculated by PONDR[28], DISOclust[29, 30], ESpritz[31]. The possibility to form protein droplets via liquid-liquid phase separation is also predicted byFuzDrop[32]. To verify the outcomes of computational calculation, reflectin proteins were introduced into HEK-293T cells.

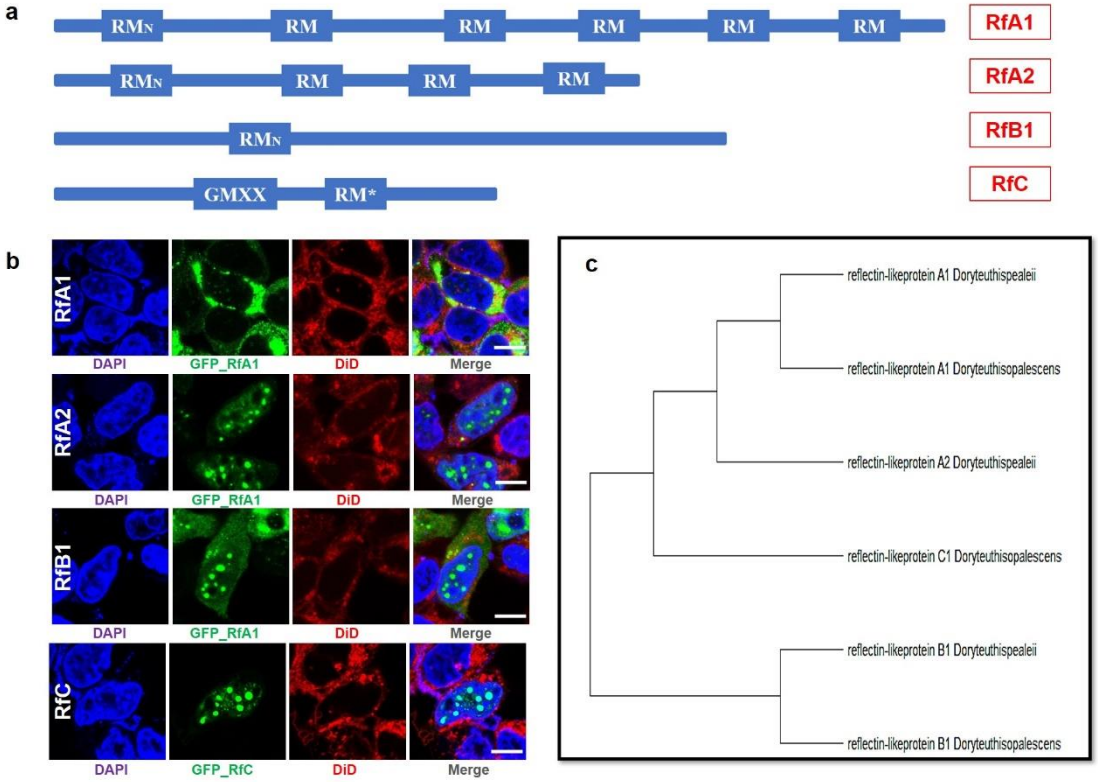

Fig.2 Transfection of reflectins induces protein condensates formation in either cytoplasm or nucleoplasm respectively. a Schematic Reflectin motifs. Reflectin Motifs are designated by boxes, while reflectin linkers (RLs) are lines. **b** Confocal images of GFP_Reflectin condensates in HEK-293T cells. Nuclei and membrane were stained with DAPI (blue) and DiD (red) respectively. **c** cladogram of RfA1, RfA2, RfB1 and RfC.

After transfection and culturing for 12hr. Protein condensates were observed in all groups. However, their difference is more significant. For RfA1, protein condensates exclusively enriched in the cytoplasm. As a sharp contrast, the extremely spherical RfC droplets only locate in the nucleoplasm. While the distribution preference of RfA2 and RfB1 seems to stay in a middle state: spherical protein droplets mainly existed in the nucleus, and minority proteins stay in the cytoplasm.

Being members of the reflectin protein family, all RfA1, RfA2, RfB1, RfC phase out from the cytoplasm or nucleoplasm. Nevertheless, they also have diverse behaviors, including but not limited to the cyto-/nucleoplasmic localization preference presented here.

According to the hypothesis raised by Can Xie, reflectin genes in cephalopods come from a transposon in symbiotic *Vibrio fischeri*[11]. The repeats of conserved motifs in reflectin sequences could be the results of transposon self-replication. In this case, it is reasonable to speculate that reflectins with different motifs represent molecules in different evolution stages, while shorter ones with simpler sequence structure should be earlier ancestors.

From this point, RfC with only a GMXX motif and RM* should be the parental protein, while the RfA1 with a RM_N and five RM is the offspring protein. Although the amino acid compositions of those motifs have changed substantially after million years of evolution, these conservative boxes in reflectin sequences may still have some correlation, or share function similarities. Based on this consideration, we started to construct truncations by cutting off the RMs from the RfA1 one by one, to make them structural comparable to RfC and to investigate their intracellular performance.

Phase separation and intracellular localization preferences of RfA1 truncations. Six pairs of primers were designed to clone the DNA sequences from RfA1 CDS. The PCR products responsible for coding of six peptides, including RM_N, RM_{Nto1}, RM_{Nto2}, RM_{Nto3}, RM_{Nto4}, and RM_{Nto5} (schematics shown in Fig. 3b), are subsequently ligated to the vector pEGFP-C1. After transfection, the expressions of GFP-tagged RfA1 truncations were validated by anti-GFP Western blotting (Fig. 3c). The molecular weights of truncations were calculated by Expod.

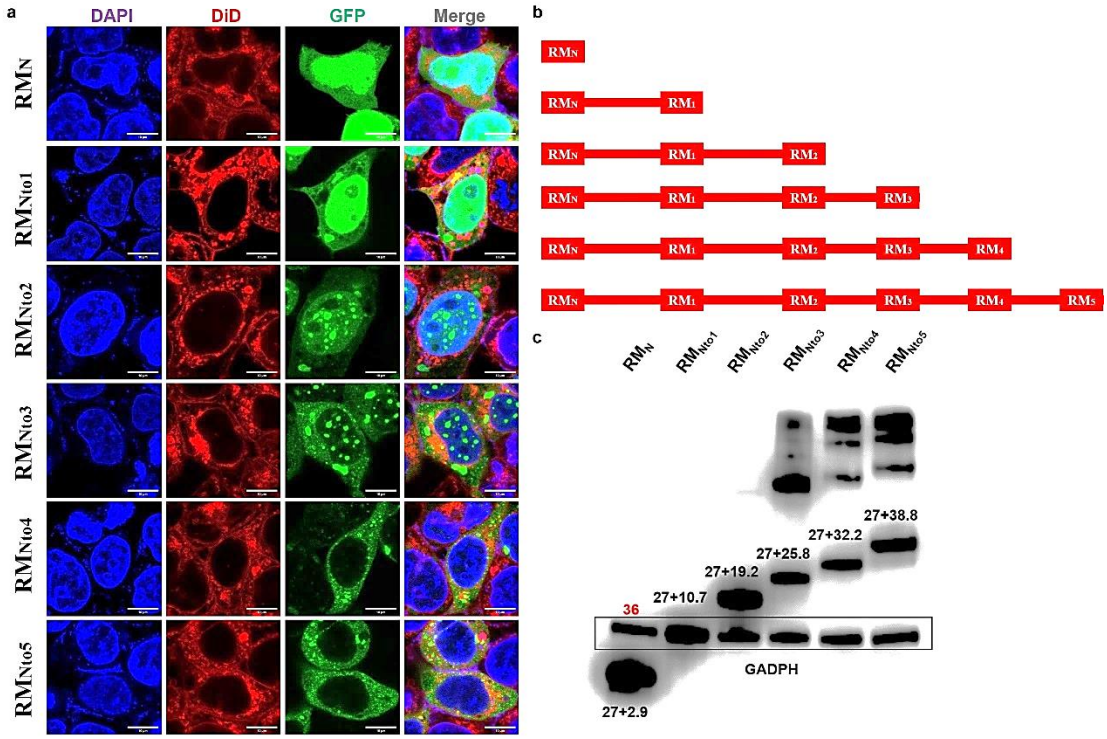

Fig.3 Expression of RfA1 truncations in HEK293T cells. a Phase separation and cyto-/nucleo-localization preferences of truncated RfA1 derivatives. Nuclei and membrane are stained with DAPI (blue) and DiD (red), RfA1-derived peptides are indicated by tandem EGFP (green). **b** schematics of RfA1 truncations. **c** the expression of RfA1 truncations were validated by Western blotting, indicated by anti-GFP antibodies. MV of EGFP is 27 kDa; GADPH is 36 kDa.

Afterward, the expression and distribution of GFP-tagged RfA1 truncations was observed by confocal image system (Fig. 3a). Nuclei and membrane are stained with DAPI (blue) and DiD (red), RfA1-derived peptides are indicated by tandem EGFP (green). For cells transfected with pEGFP-C1-RM_N and pEGFP-C1-RM_{Nto1}, though the peptide condensation seems absent, a remarkable enrichment of green fluorescence signal appears in nucleus areas. Amazingly, this nucleus-enrichment is executed more thoroughly by RM_{Nto2}, along with the recurrence of phase separation. Ulteriorly increase of conserved motifs, RM_{Nto3} are found to distribute in both cyto- and nucleo-plasm. For longer derivatives with more motifs, droplets of RM_{Nto4} and RM_{Nto5} located exclusively in cytoplasmic localization, extremely resemble their template RfA1.

For all the RfA1 truncations, RM_{Nto2} is most similar to RfC, which undergoes LLPS exclusively in nucleoplasm. More significantly, RM_{Nto2} is also a distinct boundary: truncations shorter than RM_{Nto2} tend to enrich in nuclei, but cannot form droplets; derivatives longer than RM_{Nto2} start to escape from the nuclei, and accumulate and condensate into droplets in cytoplasm.

Also noteworthy are smears in lanes of RM_{Nto3}, RM_{Nto4}, and RM_{Nto5} in Fig. 3c. These are not

sample contaminations or non-specific labeling. CoIP-MS results indicate various components tightly interact with these peptides, assisting their phase separation and causing their cytoplasmic retention.

Identification of the RfA1/RM_{Nto2} interacting proteins in HEK-293t Cells. To explore the mechanism underlying phase separation and intracellular distribution of RfA1 derivatives, a monoclonal antibody of GFP was prepared and a CoIP-MS approach was used to identify RM_{Nto2} and RfA1 protein-protein interactions (PPIs).

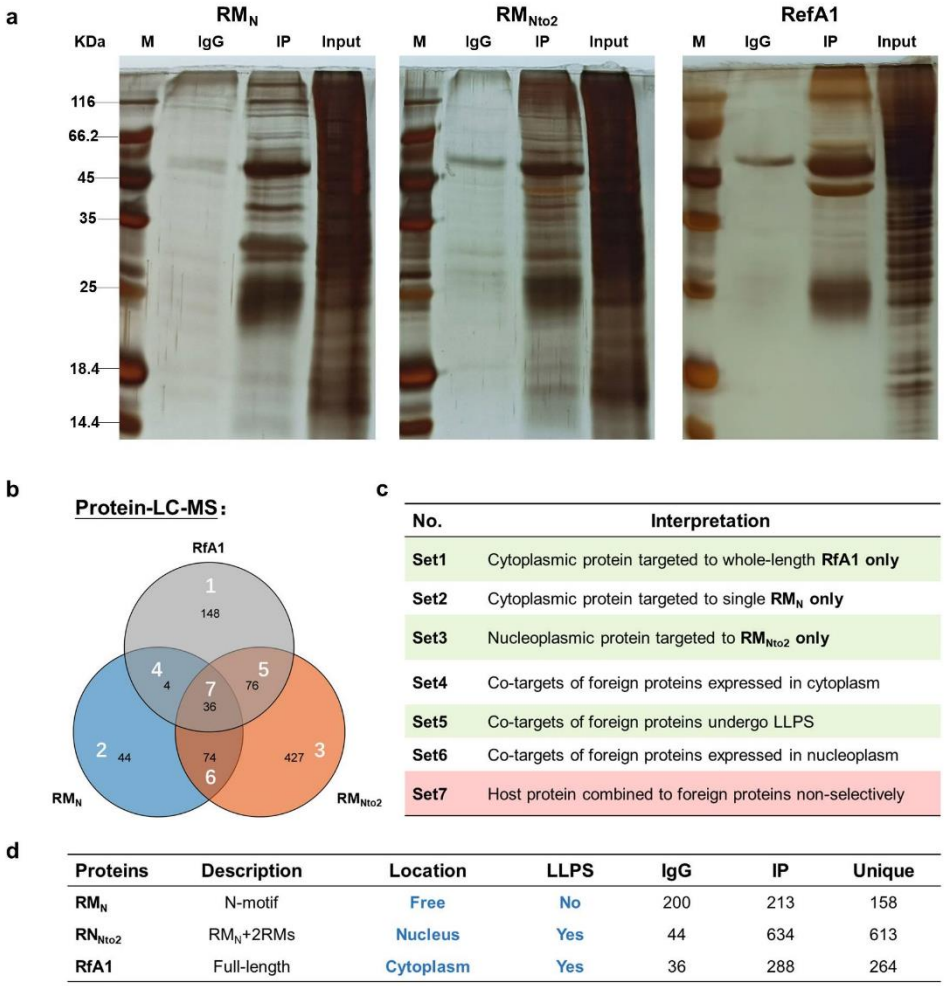

Fig.4 Identification of interactions proteins targeted to RfA1 truncations. a silver staining of IP products, whole "IP" bands will be sent to LC-MS. **b** the intersection of three LC-MS results was shown in the Boolean graph. **c** interpretations of areas in the Boolean graph. **d** PPI summary. Unique(RM_{Nto2})=IP(RM_{Nto2})－IP(RM_{Nto2})∩IgG (RM_{Nto2})－IP(RM_N)∩IgG (RM_N); Unique(RfA1)= IP(RfA1)－IP(RfA1)∩IgG (RfA1)－IP(RM_N)∩IgG (RM_N).

Aforementioned, there must be a massive interaction between RfA1 truncations and host cell proteins, resulting in the smears presented in Fig. 3c. Therefore, valuable information will be lost if only one single band was collected and analyzed. However, mixed samples consists of multiple bands inevitably bring in meaningless miscellaneous proteins. Based on these considerations, cells expressed RM_N was selected as a control (Fig. 4a) since RM_N presented no phase separation or exclusive distribution behavior.

As shown in the Boolean graph (Fig. 4b), overlays Set4/6/7 will be deducted as backgrounds, while discussions will be focused on Set1/3/5. Within Set1 are the proteins combined to whole-length RfA1, and contribute to the phase separation and cytoplasmic localization; proteins in Set3

promote the importation of truncated RM_{Nto2} into nuclei and its phase out from the nucleoplasm; co-targets of RM_{Nto2} and RfA1 are sorted into Set 5 (Fig. 4c). Protein-protein interactions are summarized in Fig. 4d.

To explore biological processes associated with RfA1 and RM_{Nto2} interacting proteins, Gene Ontology (GO) annotation analysis was performed. After screening the Biological Process (BP) lists, items of interests with adjusted p-value$<$0.05 are profiled and shown in Fig. 5a.

Take Set1-1 for example, since RfA1 interacted with proteins like HNRNPA1 [33, 34], SRSF1[35] and RAN [36, 37] and participate in process including "protein export from nucleus", it is comprehensible that the RfA1 droplets are exclusively distributed in the cytoplasm. Similarly, RANBP2[38] and various NUPs[39] in Set3-5 facilitate the importation of RN_{Nto2} into nuclei. One remarkable common points of Set1-2, Set5-3 and Set3-4 is the involvement of "ribonucleoprotein complex" or "ribonucleotide metabolic". The interaction with ribonucleoprotein complexes brings in a massive interplay with proteins and mRNA[40, 41], leads to an almost inevitable phase separation. This is consisted with results in Fig. 3. However, the involvement of ribonucleoprotein complex makes the situation even more elusive. It is hard to say whether RfA1/RN_{Nto2} molecules gathered together and phase out from the surrounding by their own properties, or they were drawn into the formation of ribonucleoprotein complex bodies.

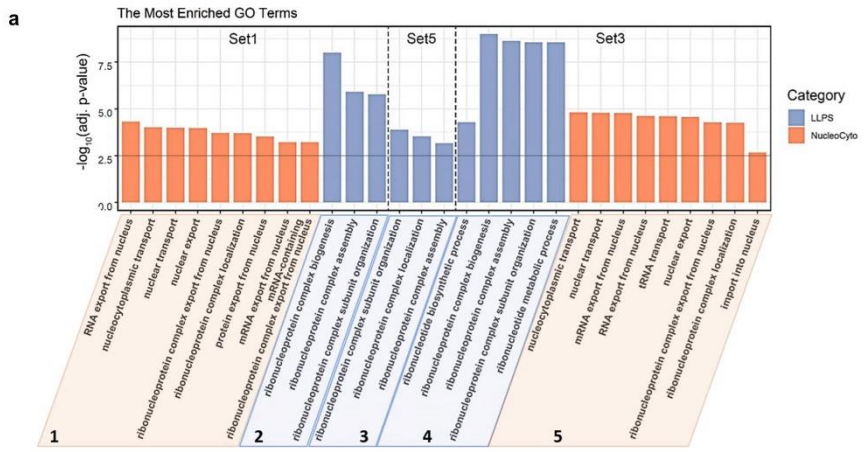

Fig.5 GO biological processes annotation of proteins associated with LLPS and cellular localization, in Set1, Set5 and Set3.

Moreover, PPI information obtained by CoIP-MS also demonstrates that RfA1 extensively interacts with actin and actin binding proteins (ABPs) (Fig. 6a, Set1-1). These proteins are in charge of various essential biological processes, including actin polymerization, nucleate assembly of new filaments, promote elongation, cap barbed or pointed ends to terminate elongation, sever filaments, and crosslink filaments [42, 43]. By cooperating with these actin and ABPs, RfA1 is likely to participate in the organization of the cytoskeleton system, thus regulates the cell morphogenesis and movement. Although there is a huge difference between HEK-293T cells and squids iridocytes, considering the evolutionarily conservative of actins among algae, amoeba, fungi, and animals [44, 45], results presented here suggest that RfA1 plays fundamental roles in the establishment and regulation of Bragg lamellae via its collaboration with cytoskeleton.

In curiosity of the relationship between reflectin proteins and membrane, proteins in Set1-2, Set5-3, Set3-4 were investigated. However, proteins are mainly RPLs and RPSs [46], which stands for the protein expression processes. The affinity of reflectins to cytomembrane is still dubious.

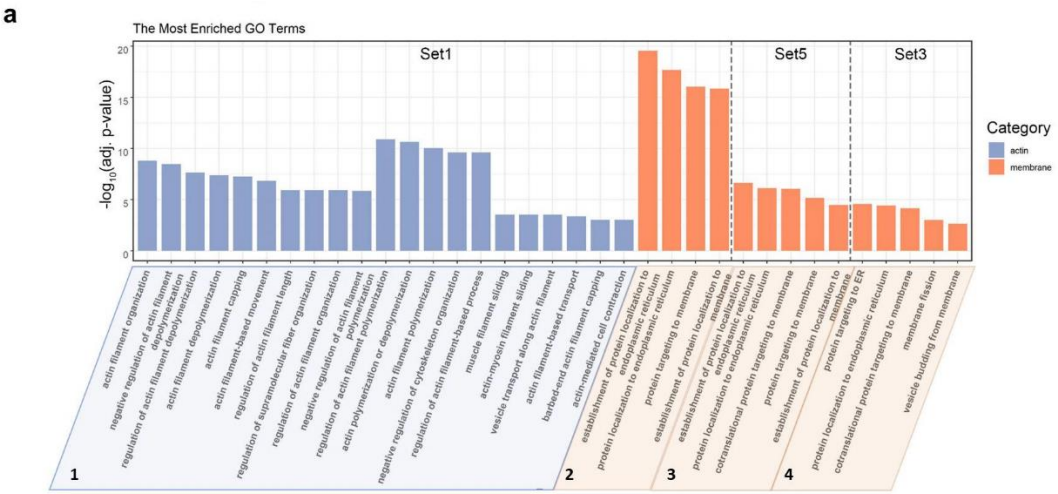

Fig.6 GO biological processes annotation analysis of proteins associated with actin and membrane systems, in Set1, Set5 and Set3.

Verification of Co-localization between RfA1 and Actin. As previously mentioned, cytoskeleton is indispensable for either the establishment or the regulation of delicate Bragg reflectors in iridocytes. However, so far, except for the Co-IP assay in this work, no evidence has been issued about the interaction between reflectin proteins and the cytoskeleton system. As a preliminary start, we stained the HEK-293T cells with ActinRed 555 (Thermo) to trace the actin network, and to verify the potential relationship between RfA1 and the cytoskeleton system. One notable trouble is the ubiquity of the actin work. It is hard to judge the co-localization of RfA1 and actin. However, after a close-up view of thousands of cells, we found an interesting scenario. For plenty of transfected cells (about 10%), there is always a bright green sphere in the center or on the central axis. Without question, these spherical balls are condensates of RfA1 (Fig. 7, GFP channel). Around these green balls, the red signal of stained actin is also significantly stronger than other areas (Fig. 7, ActinRed channel), indicating their co-localization or even the interaction. This also explains the results in Fig.2 b: the reason why GFP_RfA1 is not regular and perfectly spherical is because of their interaction with actin system. Furthermore, another phenomenon that has to be mention is that these green condensates were all found in dividing cells, which nucleus have already duplicated and begun to separate. Considering the spatial and temporal appearances, RfA1 is likely to cooperate with the centrosomes in these situations, to regulate the recruitment and movement of the whole cytoskeleton. Although systematic studies are required, these phenomena suggested that RfA1 is a qualified candidate to manipulate the cytoskeleton and the Bragg reflectors in squids.

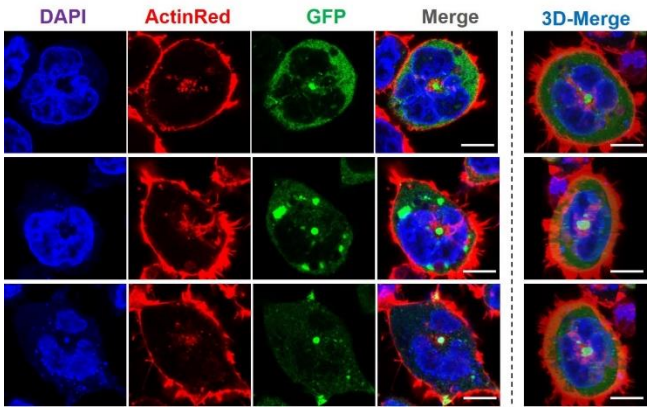

Fig.7 Appearance of spherical RfA1 condensates in the center or on the central axis of transfected cells.

Discussion

In summary, by taking advantage of reflectins natural block sequences, we realized the expression of two native reflectins (RfA1 and RfC) and six RfA1 truncations in human cells, and found their tunable phase separation and cyto-/nucleoplasmic localization preference. We believe there are multiple reasons to support the scientific significance of this work.

Firstly, the cyto-/nucleo-plasmic localization preference presented here could be an evidence for the molecular evolution of reflectin proteins. According to Can Xie's hypothesis, reflectin genes in cephalopods come from a transposon in symbiotic *Vibrio fischeri*[11]. Afterward, million years of replication and jumping of this transposon results in the formation of reflectins with different length, different motifs and different properties [3, 9, 10, 47]. In this study, longer RfA1 consists of one RM_N and five RMs exclusively enriched in cytoplasm, while RfC contains only one GMXX and a RM* stayed in nucleus. By truncating RfA1 gradually, shorter peptide derivatives (e.g., RM_{Nto2}) started to localize to nucleus, behaved exactly similar to RfC. In this case, shorter and simpler RfC should originally emerge as the ancestor molecular, in nucleus. Afterward, longer reflectins begin to be assembled and escape from the nucleus into cytoplasm (Fig. 7a), to interact with membrane and cytoskeleton systems.

Secondly, our work demonstrated that liquid-liquid phase separation is the common strategy applied by reflectins and their derivatives to achieve spatial enrichment. This is consistent with Daniel E. Morse systematic *in vivo* assays[10, 12, 47]. Phase separation leads to the condensation of functional molecules, making it possible to coordinate with other cellular components and accomplish complicated cell functions[20, 48, 49]. CoIP-MS bioinformatics investigation further revealed the extensive involvement of RfA1 into the cytoskeleton system. Considering the fundamental role of LLPS in the actin and microtubulin assembly and cytoskeleton [50], condensates formed by reflectins could be the central pivots to manipulate plasma membrane and cytoskeleton, and to fabricate the intricate Bragg lamellae in iridocytes (Fig. 7b).

Thirdly, reflectins are natural block copolymers, as well as programmable biomaterial. Their phase separation or extent of condensation could be easily adjusted by the tunable sequence length, making them potential reporters for phase microscopy. Also, if we take GFP as molecular cargoes, reflectin derivatives can be intelligent vehicles to transport cargoes to pre-designed destinations (e.g., cytoplasm or nucleus, Fig. 7c).

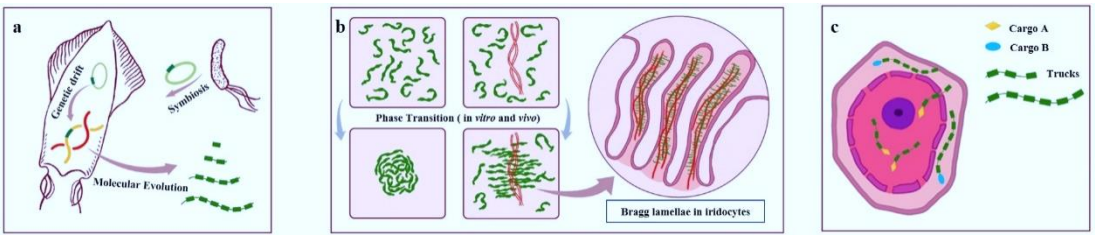

Fig.8 Models. a potential origin and evolution of reflectin proteins. **b** LLPS of RfA1 in *vitro* and *vivo*. **c** schematic diagram for RfA1 derivatives as programmable and oriented cargo carriers.

Since native cephalopod skin cells remain quite challenging to culture[26], the inevitable drawback of this work is the employment of human cell HEK-293T as the platform. We will optimize and repeat the aforementioned experiments when culture system and engineering technology to manipulate cephalopod skin cells is available. However, considering universal principles of LLPS and evolutionarily conservative of cytoskeleton among animals, results and conclusions of this work are nonetheless inspiring and valuable.

Methods

Construction of recombinant pEGFP-C1 vectors. Nucleotide sequence of *D. (Loligo) pealeii* reflectin A1 (RfA1) (Genbank: ACZ57764.1) and *D. (Loligo) Opalescens* reflectin C (Genbank: AIN36559.1) were optimized for human cell expression, then synthesized and sequencing-identified by Sangon Biotech® (Shanghai, China) Primers (F-GAATTCTATGAATAGATATTTGAATAGACA; R-GGATCCATACATATGATAATCATAATA ATTT) were designed to introduce *EcoR I* and *BamH I* cutting sites, so the modified RfA1 CDS can be constructed into pEGFP-C1 via a standard restriction enzyme cloning process. As for truncated RfA1 derivatives, six pairs of primers were coupled used. Take this for example, if RM_N-F and RM_3-R primers were selected, then a nucleotide sequence responsible for the coding of RM_N-RL_1-RM_1-RL_2-RM_2-RL_3-RM_3 (which is simplified as RM_{Nto3} in this paper) will be obtained after PCR. In the meanwhile, 5' GCATGGACGAGCTGTACAAG 3' and 5' TTATGATCAG- TTATCTAGAT 3' were added to those F-primers and R-primers respectively during primers synthesis, which enables sequences to be ligated to pEGFP-C1 by Ready-to-Use Seamless Cloning Kit from Sangon Biotech® (Shanghai, China).

Growth and transfection of human cells. HEK-293T cells (ATCC®, CRL-3216™) were cultured on plastic dishes in Dulbecco's Modified Eagle Medium (DMEM, Gibco™) supplemented with 10% fetal bovine serum (FBS, Gibco™) at a temperature of 37 °C and under 5% CO_2. One day before transfection, cells were seeded at ~33% of the confluent density for the glass bottom dishes from Cellvis (California, USA), and grown for another 24 h. Then transfection mixture containing Lipofectamine 3000 (Thermo Scientific) and recombinant vectors was added to the medium, incubating for ~16 to ~24 h. For CCK-8 tests, 1×10^4 cells were seeded into each hole of 96-well plates one day before transfection, then transfected with recombinant vectors and incubated for another 24 h. After that, 10μl of CCK-8 solution will be added into wells for a ~2 to ~4 h chromogenic reaction. OD_{450} was detected by Multiskan FC (Thermo Scientific).

Fluorescence microscopy of stained cells. Transfected HEK-293T cells grown in Cellvis plastic dishes were firstly fixed with 4% paraformaldehyde at room temperature for 30 mins, then stained with DiD (diluted in 0.5% triton X-100 PBS) for ~20 mins after PBS rinses. After washing off the fluorescent dye with PBS, fixed cells will be embedded in DAPI-Fluoromount (Beyotime, Shanghai, China) and characterized with a Leica TCS SP8 imaging system in fluorescence imaging mode. The resulting images were analyzed with ImageJ (Java 1.8.0_172/1.52b)[51] .

Online computational prediction tools. Disorder prediction of RfA1 and derivatives were conducted with PONDER® (http://www.pondr.com/), DISOclust (http://www.reading.ac.uk/bioinf-/DISOclust/) and ESpritz (http://protein.bio.unipd.it/espritz/). The probability undergoes liquid-liquid phase separation was calculated by FuzPred (http://protdyn-fuzpred.org/)

SDS-PAGE, Western Blotting. Total proteins of cells were extracted by Immunoprecipitation Kit (Sangon). Protein samples were separated in SDS-PAGE and transferred to polyvinylidene fluoride (PVDF) filter membranes (Millipore, USA) for immune-hybridization. After 1 hour blocking in PBST (phosphate buffered saline containing 0.05% Tween-20 and 2.5% BSA), the membranes were incubated with one of the following primary antibodies with corresponding concentration: anti-GFP mouse monoclonal antibody (Sangon), anti-GAPDH mouse monoclonal

antibody (Sangon). Subsequently, band visualization was performed by electro-chemiluminescence (ECL) and detected by Digit imaging system (Thermo, Japan).

In-gel digestion. For enzymolysis in protein gel (gel strip, protein solution, protein freeze-dried powder), using a clean blade to dig out the strip of interest and cut it into 0.5-0.7 mm cubes. After decolorizing with test stain/silver staining decolorizing solution, wash the rubber block with 500μL of acetonitrile solution three times until the rubber particles are completely white. Add 500 μL of 10 mM DTT, water bath at 56°C for 30 min, low-speed centrifugation for reduction reaction;add 500 μL of decolorizing solution, mix at room temperature for 5-10 min, wash the gel spots once, centrifuge at low speed to discard the supernatant; quickly add 500 μL 55 mM IAM, placed in a dark room at room temperature for 30 minutes; centrifuge at low speed for alkylation reaction,then add 500 μL of decolorizing solution, mix at room temperature for 5-10 minutes, wash the gel spots once, centrifuge at low speed, and discard the supernatant; then add 500 μL of acetonitrile until the colloidal particles are completely white, vacuum dry for 5 min. Add 0.01 μg/μL trypsin according to the volume of the gel, ice bath for 30 min, add an appropriate amount of 25 mM NH_4HCO_3 in pH8.0 enzymatic hydrolysis buffer, and enzymatic hydrolyze overnight at 37°C. After the enzymolysis is completed, add 300 μL extract, sonicate for 10 min, centrifuge at low speed, collect the supernatant, repeat twice, combine the obtained extracts and vacuum dry.

Zip-tip Desalting. Dissolve the sample with 10-20 μL 0.2% TFA, centrifuge at 10,000 rpm for 20 min, and wet the Ziptip 15 times with a wetting solution. Equilibrate with a balance solution 10 times. Inhale the sample solution for 10 cycles. Blow 8 times with rinse liquid. Note: To avoid cross-contamination, aliquot 100 μL of flushing solution per tube, and use a separate tube for each sample. Add 50 μL of eluent to a clean EP tube, and pipette repeatedly to elute the peptide. Drain the sample.

LC-MS/MS Analysis. The peptide samples were diluted to 1 μg/μL on the machine buffet. Set the sample volume to 5μL and collect the scan mode for 60 minutes. Scan the peptides with a mass-to-charge ratio of350-1200 in the sample. The mass spectrometry data was collected using the Triple TOF 5600 +LC/MS system (AB SCIEX, USA). The peptide samples were dissolved in 2% acetonitrile/0.1%formic acid, and analyzed using the Triple TOF 5600 plus mass spectrometer coupled with the Eksigent nano LC system (AB SCIEX, USA). The peptide solution was added to the C18 capture column (3 μm, 350 μm×0.5 mm, AB Sciex, USA), and the C18 analytical column (3 μm, 75μm×150) was applied with a 60 min time gradient and a flow rate of 300 nL/min. mm, Welch Materials, Inc) for gradient elution. The two mobile phases are buffer A (2% acetonitrile/0.1%formic acid/98% H2O) and buffer B (98% acetonitrile/0.1% formic acid/2% H2O). For IDA (Information Dependent Acquisition), the MS spectrum is scanned with anion accumulation time of 250 ms, and the MS spectrum of 30 precursor ions is acquired with anion accumulation time of 50 ms. Collect MS1 spectrum in the range of 350-1200 m/z, and collect MS2 spectrum in the range of 100-1500 m/z. Set the precursor ion dynamic exclusion time to 15 s.

All data needed to evaluate the conclusions in the paper are present in the paper and/or the supplementary information. All other relevant data are available from the authors upon reasonable request.

Acknowledgements

We acknowledge Prof. L. Qiu and Prof. Q. Liu (MBL, HNU), for valuable discussion. We are grateful to the National Natural Science Foundation of China (Grants 31971291) and Natural Science Foundation of Hunan Province (Grants S2020JJQNJJ1684) for their financial support. J. Song gives his personal thanks to Prof. D.E. Morse and R. Levenson (MCDB, UCSB), for their devoted guidance from 2016 to 2018.

Author contributions

J.S. designed and performed experiments, analyzed data, and completed the manuscript. C.L designed and performed experiments, analyzed the LC-MS data. L.Z. assisted in directing graduate students to carry out experiments. B.L. and L.L. performed experiments. Z.Y. analyzed data. T.M. designed and plotted the schematic diagrams in Fig. 1 and Fig. 8. W.W. and B.H. designed experiments and wrote the manuscript.

Competing interests

The authors declare no competing interests.

References

1. Hanlon RJCB. Cephalopod dynamic camouflage. *Curr Biol* **17**, R400-R404 (2007).
2. Hanlon R, Chiao C-C, Mäthger L, Barbosa A, Buresch K, Chubb CJPTotRSBBS. Cephalopod dynamic camouflage: bridging the continuum between background matching and disruptive coloration. **364**, 429-437 (2009).
3. Tao AR, DeMartini DG, Izumi M, Sweeney AM, Holt AL, Morse DEJB. The role of protein assembly in dynamically tunable bio-optical tissues. *Biomaterials* **31**, 793-801 (2010).
4. DeMartini DG, Krogstad DV, Morse DE. Membrane invaginations facilitate reversible water flux driving tunable iridescence in a dynamic biophotonic system. *Proc Natl Acad Sci U S A* **110**, 2552-2556 (2013).
5. Williams TL*, et al.* Dynamic pigmentary and structural coloration within cephalopod chromatophore organs. *Nat Commun* **10**, 1004 (2019).
6. Mäthger LM*, et al.* Bright white scattering from protein spheres in color changing, flexible cuttlefish skin. *ADV FUNCT MATER* **23**, 3980-3989 (2013).
7. Hanlon RT, Mathger LM, Bell GRR, Kuzirian AM, Senft SL. White reflection from cuttlefish skin leucophores. *Bioinspir Biomim* **13**, 035002 (2018).
8. DeMartini DG, Ghoshal A, Pandolfi E, Weaver AT, Baum M, Morse DEJJoEB. Dynamic biophotonics: female squid exhibit sexually dimorphic tunable leucophores and iridocytes. *J Exp Biol* **216**, 3733-3741 (2013).
9. DeMartini DG, Izumi M, Weaver AT, Pandolfi E, Morse DEJJoBC. Structures, organization, and function of reflectin proteins in dynamically tunable reflective cells. **290**, 15238-15249 (2015).
10. Levenson R*, et al.* Calibration between trigger and color: Neutralization of a genetically encoded coulombic switch and dynamic arrest precisely tune reflectin assembly. *J Biol Chem*

294, 16804-16815 (2019).
11. Guan Z*, et al.* Origin of the Reflectin Gene and Hierarchical Assembly of Its Protein. *Curr Biol* **27**, 2833-2842.e2836 (2017).
12. Levenson R, Bracken C, Bush N, Morse DE. Cyclable Condensation and Hierarchical Assembly of Metastable Reflectin Proteins, the Drivers of Tunable Biophotonics. *J Biol Chem* **291**, 4058-4068 (2016).
13. Phan L, Ordinario DD, Karshalev E, Walkup IV WG, Shenk MA, Gorodetsky AAJJoMCC. Infrared invisibility stickers inspired by cephalopods. *J MATER CHEM C* **3**, 6493-6498 (2015).
14. Dennis PB, Singh KM, Vasudev MC, Naik RR, Crookes-Goodson WJJAM. Research update: a minimal region of squid reflectin for vapor-induced light scattering. **5**, 120701 (2017).
15. Qin G*, et al.* Recombinant reflectin‐based optical materials. **51**, 254-264 (2013).
16. Ordinario DD*, et al.* Bulk protonic conductivity in a cephalopod structural protein. *Nat Chem* **6**, 596-602 (2014).
17. Phan L, Kautz R, Leung EM, Naughton KL, Van Dyke Y, Gorodetsky AAJCoM. Dynamic materials inspired by cephalopods. *Chem Mater* **28**, 6804-6816 (2016).
18. Yu C*, et al.* Adaptive optoelectronic camouflage systems with designs inspired by cephalopod skins. **111**, 12998-13003 (2014).
19. Handwerger KE, Cordero JA, Gall JGJMbotc. Cajal bodies, nucleoli, and speckles in the Xenopus oocyte nucleus have a low-density, sponge-like structure. **16**, 202-211 (2005).
20. Mitrea DM*, et al.* Methods for physical characterization of phase-separated bodies and membrane-less organelles. *J MOL BIOL* **430**, 4773-4805 (2018).
21. Schuster BS*, et al.* Controllable protein phase separation and modular recruitment to form responsive membraneless organelles. *Nat Commun* **9**, 2985 (2018).
22. Uversky VNJAic, science i. Protein intrinsic disorder-based liquid–liquid phase transitions in biological systems: Complex coacervates and membrane-less organelles. *ADV COLLOID INTERFAC* **239**, 97-114 (2017).
23. Zhao YG, Zhang HJDC. Phase separation in membrane biology: the interplay between membrane-bound organelles and membraneless condensates. (2020).
24. Zhang H*, et al.* Liquid-liquid phase separation in biology: mechanisms, physiological functions and human diseases. *Sci China Life Sci* **63**, 953-985 (2020).
25. Song J*, et al.* Reflectin Proteins Bind and Reorganize Synthetic Phospholipid Vesicles. *Langumir* **36**, 2673-2682 (2020).
26. Chatterjee A, Cerna Sanchez JA, Yamauchi T, Taupin V, Couvrette J, Gorodetsky AA. Cephalopod-inspired optical engineering of human cells. *Nat Commun* **11**, 2708 (2020).
27. Crookes WJ, Ding L-L, Huang QL, Kimbell JR, Horwitz J, McFall-Ngai MJJS. Reflectins: the unusual proteins of squid reflective tissues. *Science* **303**, 235-238 (2004).
28. Xue B, Dunbrack RL, Williams RW, Dunker AK, Uversky VNJBeBA-P, Proteomics. PONDR-FIT: a meta-predictor of intrinsically disordered amino acids. **1804**, 996-1010 (2010).
29. McGuffin LJJB. Intrinsic disorder prediction from the analysis of multiple protein fold recognition models. **24**, 1798-1804 (2008).
30. Ward JJ, Sodhi JS, McGuffin LJ, Buxton BF, Jones DTJJomb. Prediction and functional analysis of native disorder in proteins from the three kingdoms of life. **337**, 635-645 (2004).
31. Walsh I, Martin AJ, Di Domenico T, Tosatto SCJB. ESpritz: accurate and fast prediction of protein disorder. **28**, 503-509 (2012).

32. Hardenberg M, Horvath A, Ambrus V, Fuxreiter M, Vendruscolo MJPotNAoS. Widespread occurrence of the droplet state of proteins in the human proteome. **117**, 33254-33262 (2020).
33. Roy R*, et al.* hnRNPA1 couples nuclear export and translation of specific mRNAs downstream of FGF-2/S6K2 signalling. **42**, 12483-12497 (2014).
34. Michael WM, Choi M, Dreyfuss GJC. A nuclear export signal in hnRNP A1: a signal-mediated, temperature-dependent nuclear protein export pathway. **83**, 415-422 (1995).
35. Hautbergue GM*, et al.* SRSF1-dependent nuclear export inhibition of C9ORF72 repeat transcripts prevents neurodegeneration and associated motor deficits. **8**, 1-18 (2017).
36. Güttler T, Görlich DJTEj. Ran‐dependent nuclear export mediators: a structural perspective. **30**, 3457-3474 (2011).
37. Connor MK*, et al.* CRM1/Ran-mediated nuclear export of p27Kip1 involves a nuclear export signal and links p27 export and proteolysis. **14**, 201-213 (2003).
38. Zhang R, Mehla R, Chauhan AJPo. Perturbation of host nuclear membrane component RanBP2 impairs the nuclear import of human immunodeficiency virus-1 preintegration complex (DNA). **5**, e15620 (2010).
39. Cautain B, Hill R, de Pedro N, Link WJTFj. Components and regulation of nuclear transport processes. **282**, 445-462 (2015).
40. Sfakianos AP, Whitmarsh AJ, Ashe MPJBST. Ribonucleoprotein bodies are phased in. **44**, 1411-1416 (2016).
41. Mukherjee N*, et al.* Deciphering human ribonucleoprotein regulatory networks. **47**, 570-581 (2019).
42. Pollard TD. Actin and Actin-Binding Proteins. *Cold Spring Harb Perspect Biol* **8**, (2016).
43. Uribe R, Jay D. A review of actin binding proteins: new perspectives. *Mol Biol Rep* **36**, 121-125 (2009).
44. Dominguez R, Holmes KC. Actin structure and function. *Annu Rev Biophys* **40**, 169-186 (2011).
45. Gunning PW, Ghoshdastider U, Whitaker S, Popp D, Robinson RCJJocs. The evolution of compositionally and functionally distinct actin filaments. **128**, 2009-2019 (2015).
46. Saha A*, et al.* Genome-wide identification and comprehensive expression profiling of ribosomal protein small subunit (RPS) genes and their comparative analysis with the large subunit (RPL) genes in rice. **8**, 1553 (2017).
47. Levenson R, DeMartini DG, Morse DEJAM. Molecular mechanism of reflectin's tunable biophotonic control: Opportunities and limitations for new optoelectronics. *APL Mater* **5**, 104801 (2017).
48. Schmidt HB, Görlich DJTibs. Transport selectivity of nuclear pores, phase separation, and membraneless organelles. *Trends Biochem Sci* **41**, 46-61 (2016).
49. Linsenmeier M*, et al.* Dynamics of synthetic membraneless organelles in microfluidic droplets. **58**, 14489-14494 (2019).
50. Koppers M, Ozkan N, Farias GG. Complex Interactions Between Membrane-Bound Organelles, Biomolecular Condensates and the Cytoskeleton. *Front Cell Dev Biol* **8**, 618733 (2020).
51. Schindelin J*, et al.* Fiji: an open-source platform for biological-image analysis. **9**, 676-682 (2012).